URSI - RCRS 2022, IIT (Indore), India, 1 - 4 December, 2022

Post-sunset Scintillation on NavIC Signals during Equinoctial Periods of 2021-2022

Sukabya Dan[1,3], Satarupa Chatterjee[2], Swaraj Pal[1], Santanu Deb[1], Chaitali Koley[3] and Anindya Bose[1]
(1) Department of Physics, The University of Burdwan, Golapbag, Burdwan 713 104, India
(2) Department of Applied Science, RCC Institute of Information Technology, Kolkata 700 001, India
(3) Department of E&CE, National Institute of Technology Mizoram, Chaltlang, Aizawl-796 012, India

Abstract

Ionospheric scintillation is a major threat to the trans-ionospheric communication/ navigation links causing data loss, cycle slip, loss of lock in Global Navigation Satellite System (GNSS) receivers, and degradation/ disruption in navigation quality. GNSS and NavIC signals have been used for the study of the ionosphere by researchers and NavIC signals offer definite advantages for ionospheric research from India. This study presents the results of moderate to intense post-sunset scintillation cases during the autumn equinox of 2021 and vernal equinox 2022 at NavIC signals in the L5 band and S-band. In October 2021, moderate scintillation is observed in the L5 signal only on more than one NavIC satellite links. In March 2022, moderate to intense scintillation is observed in the L5 signal compared to the moderate scintillation observed in the S-Band. The results would be useful in understanding the advantages of the S-band for navigation applications.

1. Introduction

Scintillation is the severe fluctuation in electron density irregularities in amplitude and phase of radio signals that poses vulnerable threats to the trans-ionospheric communication/ navigation links causing data loss, cycle slip, loss of lock in Global Navigation Satellite System (GNSS) receivers, and degradation/ disruption in navigation quality. Scintillation also affects measurements of ionospheric parameters using trans-ionospheric satellite signals [1, 2]. GNSS signals have extensively been used for the study of ionospheric irregularities from different parts of the globe including India [3, 4]. The Indian regional navigation system, IRNSS/ NavIC is one of the components of GNSS that operates in L5 (1176.45 MHz) and S (2492.028 MHz) bands with satellites placed in Geostationary Earth Orbit (GEO) and Geosynchronous Orbits (GSO) for achieving better navigation accuracy and integrity around the Indian subcontinent. Because of the typical satellite constellation and signal frequency, NavIC offers certain advantages in the use of the signals for ionospheric probing from the Indian region [5]. Scintillation events originating by different scattering mechanisms are studied at multiple frequency bands- from VHF to L and recently at S-band have been explored under quiet geomagnetic conditions [6 and reference herein]. Works on the use of NavIC signals for ionospheric research have been reported in [7- 9], but not many reports may be found in the scintillation studies for the S-Band signals of NavIC. This paper presents a comprehensive study of ionospheric amplitude scintillations corroborating the L5 and S-band dataset in post-sunset hours during the recent equinoctial months of 2021 and 2022 from GNSS Laboratory Burdwan (GLB), The University of Burdwan, India (23.2545°N, 87.8467°E), situated just around the northern Equatorial Ionization Anomaly (EIA) crest from Indian longitude. The results presented in the study are useful in understanding the nature of scintillation occurring in the NavIC signals in L5 and S Band. The next section presents the experimental setup used for the study and the data morphology followed by the observation results, and finally, the conclusions are presented.

2. Experimental Setup

The NavIC constellation consists of 7 satellites- 3 (NavIC PRN 1C, 1F and 1G) of which are placed in geostationary earth orbit (GEO) and 4 (1B, 1I, 1D and 1E) are placed in inclined geosynchronous (IGSO) orbits as shown in Figure 1. The small variations of the Ionospheric Pierce Points (IPP) of the NavIC satellites provide the scope for probing the ionosphere in a different manner than the other global constellations where the IPPs vary continuously [5].

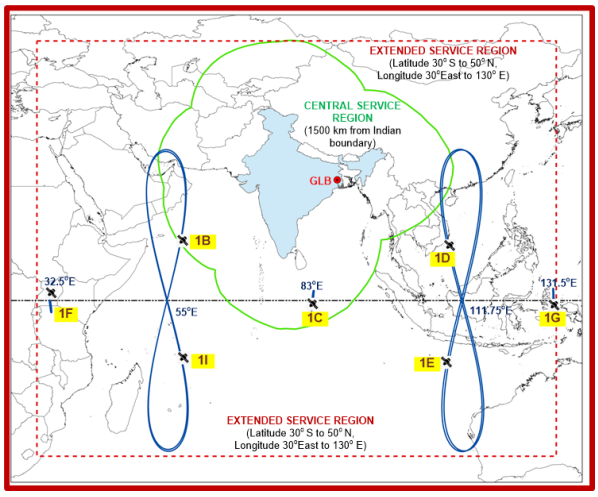

Figure 1. NavIC satellite locations, footprints and the observation location GLB, The University of Burdwan

To monitor the ionospheric activities during the equinox periods, NavIC data is recorded at GLB for L5 and S-band from September to October 2021, and March to April 2022. An ISRO-developed IRNSS-GPS-SBAS (IGS) receiver and L5+S enabled antenna placed in an obstruction-free, open-sky environment are used for the purpose as shown in Figure 2. NavIC raw data @5Hz is collected using the receiver that is converted to .csv files using a vendor-supplied software; the .csv files contain detailed navigation and satellite-related information including satellite PRN No., satellite look angles and signal strength in terms of Carrier to Noise ratio (C/N_0). DST (Disturbance Storm Time) index reveals the effect of the globally symmetrical westward flowing high altitude equatorial ring current, which causes the *main phase* depression worldwide in the H-component field during large magnetic storms. Data for geomagnetically quiet days (DST> −30 nT) are used for the present study [10].

For the present investigation, the solar radio flux at 10.7 cm (2800 MHz), usually called the F10.7 index, an indicator of solar activity, has also been considered. It is significant in specifying and forecasting space weather providing climatology of solar activity over six solar cycles. During the period of investigation, F10.7 varies in the range from 87.4 – 130.63 solar flux units (10^{-22} W m^{-2} Hz^{-1}) pertaining to higher solar flux conditions [11].

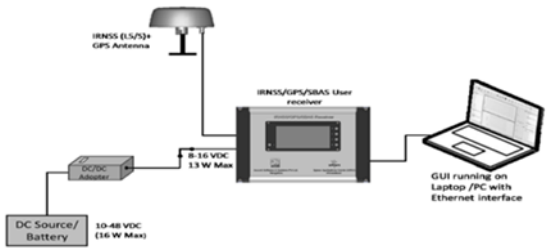

Figure 2. NavIC data collection schematic

3. Results and Discussion

Scintillation normally occurs when the Fresnel dimension of the propagating radio wave is of the order of irregularity scales in the ionosphere [12]. Deep sustained fading of amplitude severely degrades the receiver performance in addition to probable data loss for satellite links, loss of lock for the receiver, and deterioration of satellite measurements of ionospheric parameters [1].

The amplitude of signal fluctuations is directly related to the level of fluctuations in plasma density or the integrated electron density deviation ($\int \Delta N\, dl$) along the ray path. It is controlled by irregularity amplitude ($\Delta N/N$), background electron density (N) and its distribution in the ionosphere [13]. The intensity of scintillation is determined by the integrated electron density deviation of ionospheric irregularities. If the percentage deviation is the same, a higher ambient level may correspond to a larger density deviation [2]. Also, it is found that the higher solar flux condition corresponds to greater electron density in the F-region that results higher scintillation occurrence at the L-band frequencies [14] that is witnessed in the present investigation.

Study of the ionosphere using GNSS signal is done by analyzing the C/N_0 values and the derived parameters such as the S_4 index. The amplitude scintillation index, S_4, is defined as the normalized standard deviation of signal intensity over a finite period, which may be calculated from the C/N_0 values using Equation (1) shown below [12].

$$S_4 = \sqrt{\left[\frac{< S_i^2 > - < S_i >^2}{< S_i >^2}\right]} \quad (1)$$

Where $S_i = 10^{0.1 \times C/N_0}$

Here the $\langle \ldots \rangle$ brackets denote an ensemble average but in practice indicate temporal averages. S_4 is calculated over a one-minute period and the value ranges from 0 to 1; it may be greater than 1 depending on the scintillation density [15]. The three levels of scintillation as per the S_4 index are defined as weak ($0.2 \leq S_4 < 0.4$), moderate ($0.4 \leq S_4 < 0.7$), and intense ($S_4 \geq 0.7$) [16]. From the C/N_0 values of the NavIC satellite signals, the S_4 indices were calculated. The Ionospheric Pierce Points (IPP) of the satellites are calculated using the method discussed in [5].

During the Autumn equinox period of October 2021, the presence of moderate scintillation is detected at two IPPs on 23rd October 2021 in the L5 signal. For NavIC PRN 1C (GEO) for 11 minutes during 19:59- 20:10 IST at IPP: 21.6908°N, 7.4953°E with an average S_4 value of 0.252, and for NavIC 1I (GSO) at IPP 18.4830°N, 83.7257°E for 16 minutes during 21:54- 22:10 IST with an average S_4 index of 0.268 as shown in Figure 3. In the figure, the variation of C/N_0 values is also shown against the observation time in IST. Corresponding S_4 index values together with C/N_0 variations in S-band signal for the same NavIC satellite are also shown in Figure 3. It is witnessed that, during the same periods of time, no appreciable scintillation has been witnessed in the S-band; the values remain always <0.2.

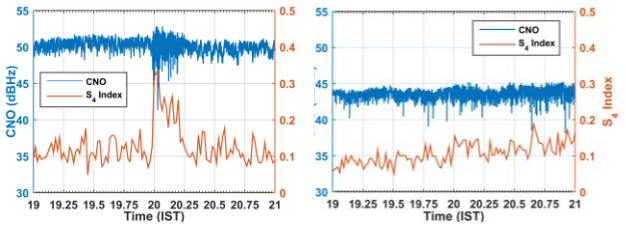

(a) for NavIC 1C

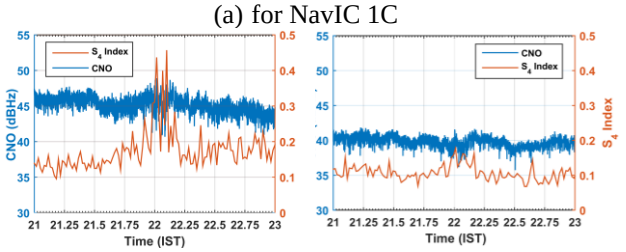

(b) for NavIC 1I

Figure 3. C/N_0 and S_4 index variation on NavIC signals in L5 (left) and S-band signals (right), 23 October 2021

Subsequently, during the Vernal equinoctial period of March 2022, simultaneous intense scintillations in the L5-band and moderate scintillation in the S-band are witnessed as shown in Figure 4 below.

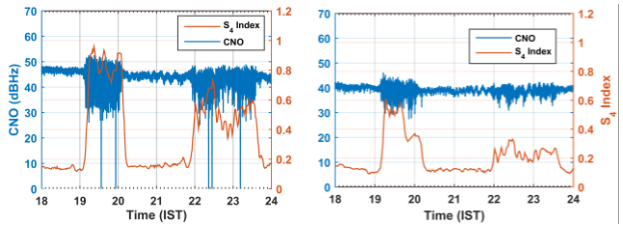

(a) For NavIC 1D

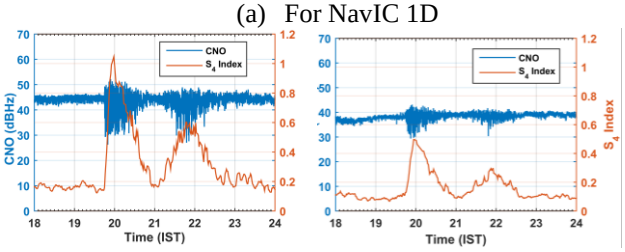

(b) For NavIC 1F

Figure 4. C/N_0 and S_4 index variation on NavIC signals in L5 (left) and S-band signals (right), 21 March 2021

During this observation period, higher scintillation occurrence features are observed than during the autumn equinox. For the NavIC L5 signal, strong scintillation is observed on 21st March 2022 for 64 minutes (19:07- 20:11 IST) for NavIC 1D (GSO) at mean IPP 19.0058°N, 89.8896°E with an average S4 index of 0.8-1.0. In addition to it, one more long scintillation patch is observed in the pre-midnight period from 21:53 IST to 23:46 IST sustaining for more than 2 hours with S4 ranging between 0.4- 0.7. For NavIC 1F (GEO) at IPP: 18.4830°N, 83.7257°E intense scintillation is registered for 68 minutes on the same day during 19:45-20:53 IST at NavIC L5 frequency. The maximum values of S4 range around 0.8-1.0. Also resembling the nature of the previous case moderate scintillation is observed from 21:13-22:44 IST, sustaining for more than 1 hour with S4 ranging between 0.5-0.6.

A very significant result compared to the October 2021 observation has been revealed for the S-band in vernal equinox time of March 2022. Moderate scintillation was concurrently observed for the NavIC 1D S-band signal on 21st March 2022 for more than 1 hour with maximum S4 values varying around 0.5-0.6 as may be observed from Figure 4. Later in the pre-midnight hours, weak scintillation has been recorded for nearly 30 minutes (22:07-22:41 IST and 23:08-23:37 IST) on the same day for the same satellite. A similar feature is observed on 21st March 2022 for the S-band signal from NavIC 1F satellite, where moderate scintillation is registered for more than 1 hour (19:48-20:33 IST) with maximum S4 values ranging around 0.4-0.5 (Figure 4). Also, a weak scintillation patch is found with S4 values <0.4 continuing for nearly 30 minutes' duration (21:40- 22:10 IST).

The presence of weak to moderate scintillation for the S-band alongside intense L band scintillation during the Vernal equinoctial month of March 2022 is of immense importance in the context of failsafe navigation, uninterrupted satellite data collection questioning the feasibility of the multi-frequency technique for efficient augmentation of satellite-based navigation services meant to provide accurate results [6].

The increased scintillation occurrence at the L5-band and the presence of the S-band scintillation during the Vernal equinox may be attributed to the higher solar flux conditions pertaining to the ascending phase of the current solar cycle 25 during the observation period. The occurrence of concurrent scintillation in both the NavIC L5 and S links at different longitudes may be attributed to the evolution of a cluster of plasma bubbles and the superposition of their effects [17] for a wide area of the overhead sky. In the S-Band, absence of scintillation during the Autumn equinox, lesser and weaker scintillation occurrences are observed during the Vernal equinox than in the L5 band. During the March 2022 observations, loss of locks of the signal at the receiver is witnessed in L5 Band (Figure 4(a)), while the S-Band maintains the lock. These suggest the relative superiority of the S-band frequency for uninterrupted communication links.

In the EIA region, the strength of ionospheric irregularities dictates the fading pattern of scintillation. The higher solar flux condition results in greater electron density in the F-region leading to enhanced scintillation activity, even at L-band frequencies [2]. Hence, the simultaneous occurrence of multi-band scintillation, especially in the S-band observed from this typical Indian location during the ascending phase of the solar cycle is of immense importance in the context of efficient augmentation of satellite-based navigation services with accuracy and integrity around the EIA crest region.

4. Conclusions

This paper presents the novel results of ionospheric scintillations observed on the NavIC L5 and S-band signals during the equinox periods of October 2021 and March 2022 from India. During October 2021, moderate scintillations in terms of the S_4 indices are observed in L5 band NavIC links, but the S-band signal remains undisturbed. Again, in March 2022, moderate to very high scintillation is observed in the L5 band links, while in the S-band, less frequent and less intense scintillation is observed during the same observation periods and the same satellite links. Loss of lock is observed in the L5 signals, while the S-band remains undisturbed from this viewpoint. The results are important in understanding the scintillation events for the Indian region using NavIC signals problems in multifrequency scintillation, and the relative superiority of the S-band for navigation applications during such intense ionospheric events. Future work in this respect would be the analysis of data collected during equinox periods from multiple locations and the use of compact,

low-cost, dual-frequency receiver modules for NavIC-based ionospheric research from India.

5. Acknowledgements

The authors acknowledge the financial support from DST-SERB (Project Code: CRG/2020/005098) and University Grants Commission (CAS II), and hardware support from Space Applications Centre (SAC), ISRO, Ahmedabad.

6. References

1. D. L. Knepp, "Effects of ionospheric scintillation on Transit satellite measurement of total electron content," *Radio Science*., Vol. 39, Issue 1, pp. 1-8, 2004 doi:10.1029/2002RS002825.

2. S. Chatterjee, and S. K. Chakraborty, "Variability of ionospheric scintillation near the equatorial anomaly crest of the Indian zone," *Annales Geophysicae*, Vol. 31, No. 4, pp. 697-711, 2013, doi: 10.5194/angeo-31-697-2013.

3. X. Ren, X. Zhang, W. Xie, K. Zhang, Y. Yuan and X. Li, "Global ionospheric modelling using multi-GNSS: BeiDou, Galileo, GLONASS and GPS," *Scientific reports*, Vol. 6, pp. 1–11, 2016, doi: 10.1038/srep33499.

4. P. V. S. R. Rao, S. G. Krishna, K. Niranjan and D. S. V. V. D. Prasad, "Study of spatial and temporal characteristics of L-band scintillations over the Indian low-latitude region and their possible effects on GPS navigation," *In Annales Geophysicae*, Vol. 24, pp. 1567- 1580, 2006, doi: 10.5194/angeo-24-1567-2006

5. A.K. Sharma, O.B. Gurav, A. Bose, H.P. Gaikwad, G.A. Chavan, A. Santra, S.S. Kamble and R.S. Vhatkar, "Potential of IRNSS/NavIC L5 signals for ionospheric studies," *Advances in Space Research*, Vol. 63, Issue 10, pp.3131-3138, 2019. doi: 10.1016/j.asr.2019.01.029.

6. S. K. Chakraborty, S. Chatterjee and Debasis Jana, "A study on multifrequency scintillations near the EIA crest of the Indian zone," *Advances in Space Research (Special edition)*, Vol. 60, Issue 8, pp- 1670-1687, 2017, doi: 10.1016/j.asr.2017.02.020.

7. Mehul V. Desai and Shweta N. Shah, "Estimation of ionospheric delay of NavIC/IRNSS signals using the Taylor Series Expansion," *Journal of Space Weather and Space Climate*, Vol. 9, No. A23, 2019, doi: 10.1051/swsc/2019023.

8. S. C. Bhardwaj, A Vidyarthi, B.S. Jassal, A.K. Shukla, "An assessment of ionospheric delay correction at L5 and S1 frequencies for NavIC Satellite System," *2020 Global Conference on Wireless and Optical Technologies (GCWOT)*, 2020, doi: 10.1109/GCWOT49901.2020.9391601.

9. D. Venkata Ratnam, T. Raghavendra Vishnu, P. Babu Sree Harsha, "Ionospheric Gradients Estimation and Analysis of S-Band Navigation Signals for NAVIC System," *IEEE Access*, Vol. 6, pp. 66954– 66962, 2018, doi: 10.1109/ACCESS.2018.2876795.

10. Real-time (Quicklook) Dst index, World Data Center for Geomagnetism, Kyoto. https://wdc.kugi.kyoto-u.ac.jp/dst_realtime/index.html. Accessed on 20th April 2022.

11. Space Weather Prediction Center, National Oceanic and Atmospheric Administration. https://www.swpc.noaa.gov/phenomena/f107-cm-radio emissions. Accessed on 15th April, 2022.

12. B.H. Briggs and I.A. Parkin, "On the variation of radio star and satellite scintillations with zenith angle," *Journal of Atmospheric and Terrestrial Physics*, Vol. 25, Issue 6, pp.339-366, 1963, doi: 10.1016/0021-9169(63)90150-8.

13. S. Basu, E. MacKenzie and S. Basu, "Ionospheric constraints on VHF/UHF communication links during solar maximum and minimum periods," *Radio Science*, Vol. 23, Issue 3, pp. 363–378, 1988, doi: 10.1029/RS023i003p00363.

14. J. Aarons, H. E. Whitney, E. MacKenzie, and S. Basu, "Microwave equatorial scintillation intensity during solar maximum," *Radio Science*, Vol. 16, Issue 5, pp. 939–945, 1981, doi: 10.1029/RS016i005p00939.

15. J.M. Juan, A. Aragon-Angel, J. Sanz,G. González-Casado and A. Rovira-Garcia, "A method for scintillation characterization using geodetic receivers operating at 1 Hz," *Journal of Geodesy*, Vol. 91, pp.1383-1397, 2017, doi: 10.1007/s00190-017-1031-0.

16. A.O. Akala, P.H. Doherty, C.E. Valladares, C.S. Carrano and R. Sheehan, "Statistics of GPS scintillations over South America at three levels of solar activity,". *Radio Science*, Vol. 46, Issue 5, pp.1-16, 2011, doi: 10.1029/2011RS004678.

17. C.S. Huang, O. de La Beaujardiere, P.A. Roddy, D.E. Hunton, J.O. Ballenthin, M.R. Hairston, "Generation and characteristics of equatorial plasma bubbles detected by the C/NOFS satellite near the sunset terminator," *Journal of Geophysical Research: Space Physics*, Vol. 117, Issue A11, 2012, doi: 10.1029/2012JA018163.